PHYSICAL REVIEW C **79**, 061602(R) (2009)

Isoscaling of fragments with $Z = 1$–17 from reconstructed quasiprojectiles

S. Wuenschel,[1,2,*] R. Dienhoffer,[2,3] G. A. Souliotis,[2] S. Galanopoulos,[2,†] Z. Kohley,[1,2] K. Hagel,[2] D. V. Shetty,[2,‡] K. Huseman,[2] L. W. May,[1,2] S. N. Soisson,[1,2] B. C. Stein,[1,2] A. L. Caraley,[3] and S. J. Yennello[1,2]

[1]*Chemistry Department, Texas A&M University, College Station, Texas 77843, USA*
[2]*Cyclotron Institute, Texas A&M University, College Station, Texas 77843, USA*
[3]*Department of Physics, State University of New York at Oswego, New York 13126, USA*

(Received 9 February 2009; revised manuscript received 3 May 2009; published 10 June 2009)

In heavy-ion collisions, isoscaling provides a method for studying the evolution of nuclear symmetry energy as a function of excitation energy. One challenge in using isoscaling is to accurately determine the neutron-to-proton ratio (N/Z) of the fragmenting source. Isoscaling results are presented for the reactions of ^{86,78}Kr + ^{64,58}Ni at 35 MeV/nucleon taken on the NIMROD-ISiS array at Texas A&M University. The N/Z of the source was calculated from the isotopically identified fragments and experimentally measured neutrons emitted from reconstructed quasiprojectiles. These data exhibit isoscaling for elements with $Z = 1$–17 over a broad range of isotopes. The isoscaling parameter α is shown to increase with increasing difference in the neutron composition (Δ) of the compared sources. For a selected Δ, the ratio α/Δ is also shown to decrease with increasing excitation energy. This may reflect a corresponding decrease in the nuclear symmetry energy.

DOI: 10.1103/PhysRevC.79.061602 PACS number(s): 25.70.Pq, 25.70.Mn

Nuclear symmetry energy plays a central role in both nuclear physics and astrophysics and is currently a topic of significant theoretical and experimental study [1–3]. The value of the symmetry energy has been fairly well constrained at normal nuclear density and zero temperature. Heavy-ion reaction experiments have attempted to measure the symmetry energy at non-normal densities and elevated temperatures [4,5]. Recent measurements of neutron star radii have provided symmetry energy values that are consistent with those emerging from nuclear physics experiments [2]. In addition to nuclear skin thickness studies [e.g., Ref. [6] and references therein], the nuclear symmetry energy may be experimentally accessed through isoscaling [7,8].

In heavy-ion collisions, it has been shown that the ratio $R_{21}(N, Z)$ of the yields of a given fragment obtained from the two reactions exhibits an exponential dependence on neutron (N) and proton (Z) numbers of the fragment. This assumes a statistical fragment production mechanism in which the two reactions occur at the same temperature and differ only in their isospin asymmetry [7,9,10]. This relationship is described in

$$R_{21}(N, Z) = Y_2(N, Z)/Y_1(N, Z) = C \exp(N\alpha + Z\beta), \quad (1)$$

where α and β are the scaling parameters and C is an overall normalization constant. Traditionally, reaction 2 corresponds to the neutron-rich source and reaction 1 to the less neutron-rich source. This scaling behavior is called isotopic scaling or isoscaling [9] and has been observed in a variety of reactions under the conditions of statistical emission and equal temperature [10–14]. Additionally, isoscaling has been observed in theoretical studies employing the grand canonical ensemble [8,15], the canonical ensemble [8], the expanding emitting source [9], and molecular dynamics [16,17].

The isoscaling parameter α may be linked theoretically [8,9,12,16] to nuclear symmetry energy through

$$\alpha = \frac{4C_{\text{sym}}}{T}\left[\left(\frac{Z}{A}\right)_1^2 - \left(\frac{Z}{A}\right)_2^2\right] = \frac{4C_{\text{sym}}}{T}\Delta, \quad (2)$$

where C_{sym} is the symmetry energy coefficient of the nuclear binding energy, T is the temperature, and the Z/A (charge/mass) values correspond to the neutron richness of the two sources. As in Eq. (1), source 2 is typically the more neutron-rich and source 1 is less neutron-rich. The parameter Δ represents the difference in neutron concentration between the two sources.

Two major experimental challenges in studying isoscaling are (i) accounting for fragment secondary decays and (ii) accurately determining the neutron-to-proton ratio (N/Z) of the fragmenting source. Both of these issues can be addressed through theoretical simulations of the reactions [1,18]. An alternative employed here is to experimentally determine the N/Z of the source.

In this work, we present isoscaling results from the reactions of ^{86,78}Kr + ^{64,58}Ni at 35 MeV/nucleon taken with the NIMROD-ISiS array [19,20] at Texas A&M University. The granularity and excellent isotopic resolution provided by the array enable the reconstruction of the quasiprojectile source in both Z and A. The NIMROD-ISiS charged particle array is housed inside the TAMU Neutron Ball. The Neutron Ball provides experimental information on the free neutrons emitted during a reaction [19].

There are three possible sources of fragment charge and mass identification in NIMROD-ISiS. Pulse shape discrimination of the CsI fast versus slow light output is used for $Z = 1$, 2. The ΔE-E method is used for $Z \geqslant 3$ on Si-Si and Si-CsI. The particle identification was done through linearization of the raw data [20] to remove the nontrivial curvature due to the

*wuenschel@comp.tamu.edu
†Present address: Hellenic Army Academy, Department of Physical Sciences & Applications, Athens, Greece.
‡Present address: Physics Department, Western Michigan University, Kalamazoo 49008, MI, USA.

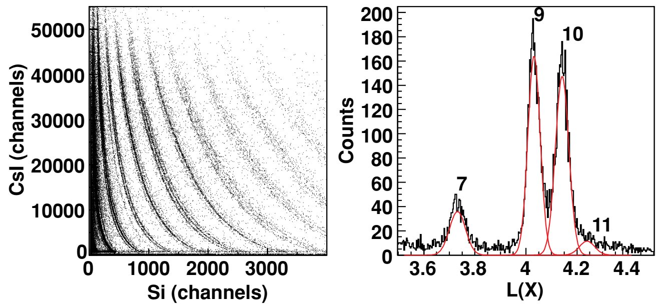

FIG. 1. (Color online) Left: Raw data from ΔE-E with Si-CsI detectors. Right: Projected, linearized data for $Z = 4$ isotopes. The x axis is L_X.

energy deposition characteristics of the detection methods (see left panel of Fig. 1). The linearization utilized lines carefully chosen to follow the strongest isotope of each element. The data were then straightened using a calculation of the distance between the data point and the two closest chosen lines. The linearized data were then projected onto a single axis and the charge assigned by limits placed on the linearization x-axis value (L_X) (see right panel of Fig. 1).

The isotopic peaks in the projected distributions were fitted with Gaussian functions. The mass of each particle was assigned by determining the probability of the particle belonging to a given isotope. This probability P_A was calculated by comparing the value of the isotopic Gaussian functions at the L_X value of the particle

$$P_A = \frac{G_A(L_X)}{\sum_i G_i(L_X)}, \tag{3}$$

where G_A is the fit to the selected isotope which is compared to the summation over all Gaussians (G_i) of the element. A nonzero mass was defined only if the probability was $\geqslant 0.75$. This method of fitting the linearized data with Gaussians provided the ability to estimate the average contamination between neighboring isotopes. The contamination in the yield of a given isotope as defined here was calculated to be $\leqslant 5\%$ across all systems and all detectors. To account for systematic errors, the yield errors in these data were taken, for a given isotope, as the larger of either the square root of the yield or 10% of the yield of the relevant isotope. This error was propagated through the fitting procedure in the functions involved.

The quasiprojectile source was selected by means of several event-by-event cuts on the experimental data. The first cut required that the sum of the collected charged fragments (sumZ) for the event equal a minimum of $Z = 30$. The fragments in an accepted event were then cut on the longitudinal velocity relative to the largest fragment [21]. This cut varied with the fragment Z. The fragments retained for $Z = 1$, $Z = 2$, and $Z \geqslant 3$ had longitudinal velocities within the range of +/− 65%, 60%, 40%, respectively, of the largest fragment longitudinal velocity. The sum of the charges of the collected and accepted fragments was again constrained to be in the range $Z = 30$–34. Limits were placed on the deformation of the source by means of a cut on the quadrupole moment of the momentum distribution.

This method of source definition was compared with events and fragments generated by the HIPSE-SIMON code [22]. The initial sumZ cut eliminated a significant number of incomplete events and events from other sources. This cut, however, was not sufficient to eliminate all fragments resulting from midvelocity or preequilibrium sources. The fragment velocity cut successfully provided a means of eliminating fragments from nonprojectile-like sources. The final cut on the deformation provided a reasonable level of isotropy in the selected events.

Isoscaling has traditionally been performed between two systems [11,23] with the N/Z of the source derived from the N/Z of the reacting systems. As shown by Rowland *et al.* [24] for midperipheral reactions, the centroid of the reconstructed quasiprojectile N/Z distribution shifts away from that of the projectile toward the valley of stability. Distributions of the reconstructed quasiprojectile N/Z can be seen in Fig. 3. The width of these distributions is large, particularly as compared to the difference in the average N/Z between the reacting systems. Isoscaling as a function of selected regions of N/Z extracted from within a system [18,25] has demonstrated that the success of isoscaling depends on accurately determining the N/Z of the source before fragmentation.

The fragment yield ratios from the reactions of ^{86}Kr + ^{64}Ni and ^{78}Kr + ^{58}Ni are shown in the top panel of Fig. 2. Each element is plotted with a different symbol, and the fit of Eq. (1) to the ratios is depicted by the solid lines. These yield ratios did not exhibit clear isoscaling. The small range of ratio values shown in this plot is a result of a small Δ between the sources.

To improve the isoscaling, the data were cut on the N/Z of the fragmenting quasiprojectile source. The N/Z was calculated by summing the number of the neutrons and protons bound in the detected charged particles:

$$\left.\frac{N}{Z}\right|_{\text{bound}} = \frac{\sum_i^{M_{cp}} N_i}{\sum_i^{M_{cp}} Z_i}. \tag{4}$$

The data from each beam/target combination were cut using N/Z_{bound} bins of 1.0–1.06 (bin 2) and 1.2–1.26 (bin 4) placed on the reconstructed quasiprojectiles to construct the neutron-poor and neutron-rich sources as required for Eq. (1). Similar isoscaling behavior was observed in each system; thus, the systems were added together to increase statistics. The ratio of the isotopic yields from the combined systems for $Z = 1$–17 as a function of neutron number is shown in the middle panel of Fig. 2 using N/Z_{bound} bins 1 and 3. All isotopes were then fit simultaneously with Eq. (1). The simultaneous fit isoscaling parameter α for this plot is 0.912, and the β parameter is -1.089. The clear improvement in the isoscaling between the top and middle panels demonstrates the sensitivity of this observable to the determination of the source N/Z.

Comparison of the top and middle panels of Fig. 2 demonstrates the improvement of isoscaling with a narrowly defined N/Z of the source. Free neutrons, belonging to the source, must be accounted for in the calculation of Δ [Eq. (2)]. Attempts have been made to account for the undetected neutrons by using a source N/Z derived from the reacting systems [11] or from theoretically corrected N/Z_{bound} [18]. These data include experimentally detected neutrons

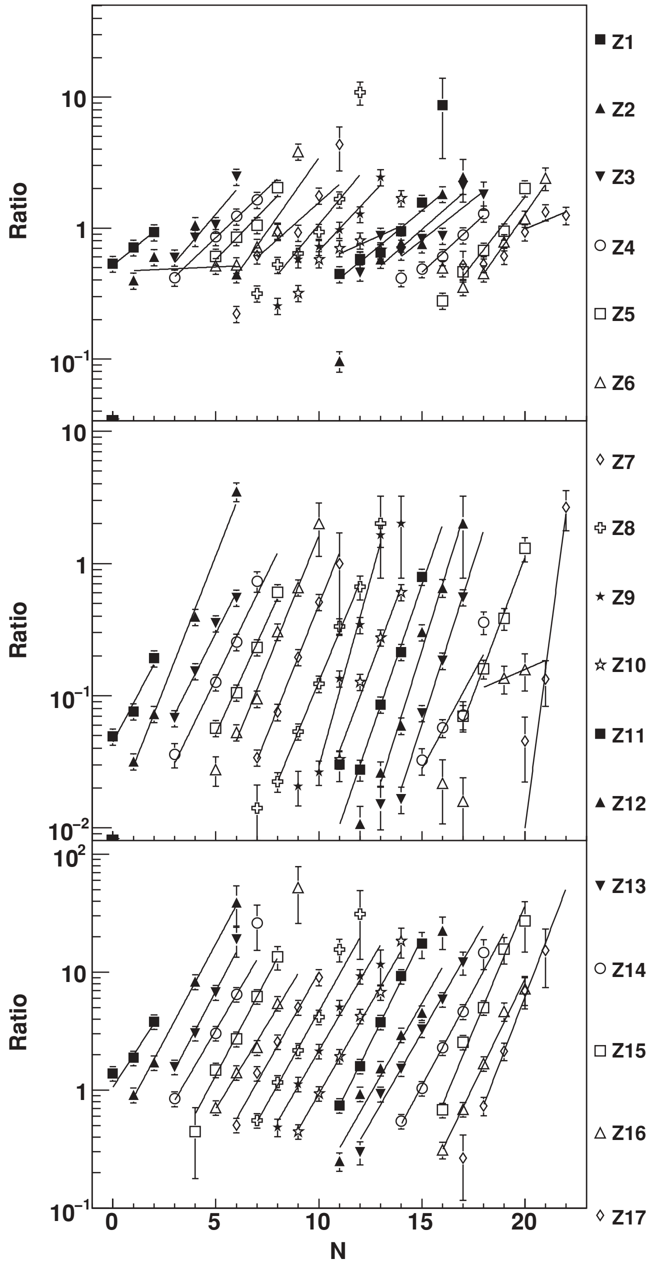

FIG. 2. Isotopic yield ratios. Top: System-to-system isoscaling ^{86}Kr + ^{64}Ni, ^{78}Kr + ^{58}Ni. Middle: Isoscaling using neutron-rich and neutron-poor bins on the reconstructed, bound N/Z of the quasiprojectile. Bottom: Isoscaling using neutron-rich and neutron-poor bins on the reconstructed, neutron-corrected N/Z of the quasiprojectile (see text).

from the Neutron Ball [19], thus allowing an experimental determination of the source N/Z:

$$\frac{N}{Z}_{\text{measured}} = \frac{\sum_i^{M_{\text{cp}}} N_i + M_n}{\sum_i^{M_{\text{cp}}} Z_i}. \tag{5}$$

The multiplicity of free neutrons was extracted from the experimental data using

$$\text{Mult}_{\text{QP}} = \frac{\text{Mult}_{\text{exp}}}{E_{\text{QP}} + \frac{N_T}{N_P} E_T}. \tag{6}$$

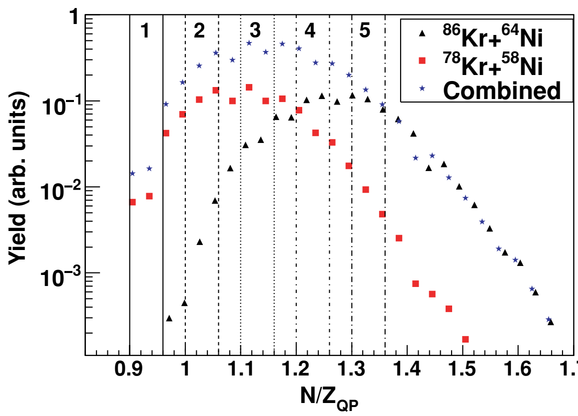

FIG. 3. (Color online) Neutron-corrected N/Z of the quasiprojectiles obtained from the ^{86}Kr + ^{64}Ni (triangles), ^{78}Kr + ^{58}Ni (squares) reacting systems. The total yield of each system was normalized to unity. The neutron-corrected N/Z of the quasiprojectiles obtained from the combined systems are plotted as stars. The total yield was normalized to 4 for this distribution. Five zones are defined with $N/Z_{\text{QP}} = 0.9$–0.96 (bin 1), 1.0–1.06 (bin 2), 1.1–1.16 (bin 3), 1.2–1.26 (bin 4), and 1.3–1.36 (bin 5).

The multiplicity of neutrons assigned to the projectile source (Mult_{QP}) was calculated from the background-corrected experimental neutron multiplicity (Mult_{exp}). This multiplicity was then corrected using the relative efficiency of the Neutron Ball for detecting free neutrons emitted from a quasiprojectile (E_{QP}) and quasitarget (E_{QT}) for this reaction. The free neutron correction also accounted for the respective total neutron contributions from both the target (N_T) and projectile (N_P) nuclei. The efficiencies were extracted from tagged neutrons generated by the HIPSE-SIMON code [22] and a GEANT3 [19] simulation of the detector. Through this formulation, only neutrons attributed to the quasiprojectile source were included. The distribution of reconstructed quasiprojectile N/Z_{measured} is plotted in Fig. 3.

To investigate the effect of the free neutron correction, bins of N/Z_{measured} equal to 1.0–1.06 (bin 2) and 1.2–1.26 (bin 4) were placed on the reconstructed quasiprojectiles from the combined systems. The resulting isoscaling is shown as the bottom panel of Fig. 2. The consistency and linearity of the elemental lines are notable, especially in light of the wide range in N-Z of the isotopes shown for each element. Each element has been fitted individually with Eq. (1), and the α obtained plotted in the right panel of Fig. 4. All isotopes were fitted simultaneously to obtain the global scaling plotted as a solid line in the right panel of Fig. 4.

It has been proposed that a strong surface dependance of the symmetry energy could be evidenced by a significant change in α as a function of fragment Z [26]. However, as shown in Fig. 4, there is no evidence in these data to support a change in the parameter α as a function of Z. On the contrary, the global scaling

$$S(N) = R_{21}(N, Z)\exp(-Z\beta) \tag{7}$$

of the yield ratios shown in the left panel of Fig. 4 shows excellent agreement with a single overall value of α (0.733)

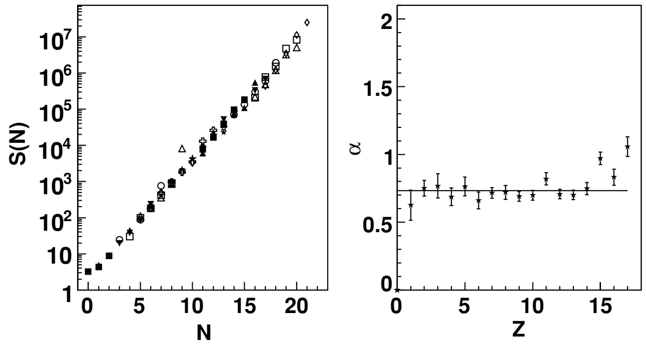

FIG. 4. Left: $S(N)$ as a function of particle neutron number. The error bars are smaller than the size of the point. Elemental symbols are the same as shown in Fig. 2. Right: Isoscaling parameter α from the fitting of the yield ratios of each Z. The global fitting α is depicted by the solid line.

and β (−0.842) obtained from simultaneous fitting of Eq. (1) for this range of Z.

From Eq. (2), it is clear that the magnitude of the α parameter depends on the difference in neutron composition (Δ) between the two sources. Five bins in N/Z_{measured} (0.90–0.96, 1.0–1.06, 1.1–1.16, 1.2–1.26, and 1.3–1.36) were defined on the reconstructed quasiprojectiles as shown in Fig. 3. Values of α were obtained by simultaneous fitting of the yield ratios across all isotopes from these bins. The Δ was obtained by averaging the Z and A of quasiprojectiles within each bin. The dependance of α on the Δ of the reconstructed source is shown in Fig. 5. An additional point is added from the isoscaling of ^{86}Kr + ^{64}Ni and ^{78}Kr + ^{58}Ni using only the neutron-corrected N/Z bin 3 for each system. The extracted α is very near zero (0.064) as would be expected from a Δ that, within experimental uncertainties, is near zero. By taking the ratio of α to the Δ of the source, the behavior of C_{sym} [Eq. (2)] with respect to excitation energy may be more easily studied.

In heavy-residue [23,27] and heavy-ion reaction [1,18] isoscaling data, it has been shown that α/Δ decreases with

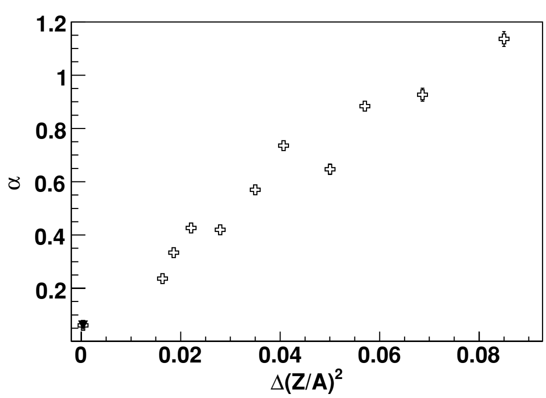

FIG. 5. Global α fits to combinations of the five bins in N/Z (0.90–0.96, 1.0–1.06, 1.1–1.16, 1.2–1.26, and 1.3–1.36) as a function of the calculated average $\Delta(Z/A)^2$ of the sources. An additional point (triangle) is added from the isoscaling of ^{86}Kr + ^{64}Ni and ^{78}Kr + ^{58}Ni using a single N/Z bin 2 for each system. The propagated error on these values, where not visible, are smaller than the size of the points.

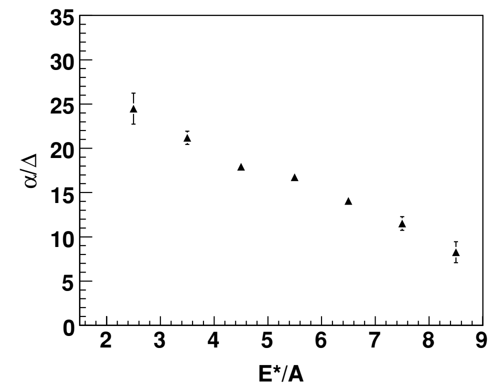

FIG. 6. Isoscaling α parameter as a function of the E^*/A (MeV) of the reconstructed source. The source N/Z bins were chosen as 2 and 4. The propagated errors, based on yield as described in the text, are smaller than the size of the points.

increasing energy of the reacting system. To examine the behavior of α/Δ as a function of the excitation energy per nucleon of the fragmenting sources, the isoscaling of the combined systems is taken from the 1.0–1.06 (bin 2) versus the 1.2–1.26 (bin 4) N/Z bin. Reconstruction of the quasiprojectile allows us to calculate the excitation energy through calorimetry:

$$E^*_{\text{source}} = \sum_i^{M_{\text{cp}}} K_{\text{cp}}(i) + M_n\langle K_n\rangle - Q. \tag{8}$$

The excitation energy (E^*_{source}) is defined as the center-of-mass kinetic energies K_{cp} summed over the accepted charged particles in the event together with the neutron multiplicity M_n multiplied by the average neutron energies $\langle K_n\rangle$ with the reaction Q value subtracted. The average kinetic energy of the neutrons was calculated as the proton average kinetic energy with a correction for the Coulomb barrier energy [28].

Figure 6 depicts the evolution of the normalized scaling parameter α/Δ as a function of the excitation energy of the reconstructed quasiprojectile using N/Z_{measured} bins of 1.0–1.06 (bin 2) and 1.2–1.26 (bin 4). The value of the α/Δ parameter is clearly decreasing as a function of increasing excitation energy. This decrease is consistent with heavy-residue and heavy-ion reaction isoscaling data [1,18,23,27] and may be indicative of a decrease in symmetry energy as a function of increasing excitation energy.

To extract the evolution of C_{sym} with E^*/A from α/Δ, the change in temperature with E^*/A must be understood. The Natowitz *et al.* [29] compilation suggests a temperature change from ∼5.5 MeV to ∼7 MeV over the E^*/A range 2.5–8.5 MeV. Using $T = 5.5$ MeV, at $E^*/A = 2.5$ MeV/nucleon, the measured α/Δ of ∼25 yields a C_{sym} ∼33 MeV. Taking this same temperature of 5.5 MeV at $E^*/A = 8.5$ MeV and an α/Δ of ∼8 yields C_{sym} ∼11 MeV. However, if the temperature has indeed increased to ∼7 MeV at $E^*/A = 8.5$ MeV the C_{sym} would become ∼14 MeV. Thus, this change in temperature can account for no more than ∼15% of the decrease in α/Δ observed here.

A drop in the nuclear symmetry energy with increasing excitation energy has been linked to a decrease in the density of the system [1,2,30]. The binary decay code GEMINI [31] was used to create a constant density baseline for $E^*/A = 2.5$–4.5 MeV. The A, Z, and E^*/A from experimentally reconstructed quasiprojectiles were used as inputs to the code on an event-by-event basis. The source angular momentum was calculated as $20(E^*/A)\,\hbar$ for $E^*/A \leqslant 3$ MeV and taken as 60 $\hbar$ for $E^*/A = 3$–5 MeV. This formula was extracted from reaction modeling with the DIT code of Tassan-Got and Stephan [32]. As in the experimental data, fragments from the source $N/Z_{\rm measured}$ bins 2 and 4 were used to construct isoscaling. Over this region in E^*/A, the GEMINI predicts a ∼15% decrease in α/Δ. The decrease in α/Δ from GEMINI can be completely accounted for by the ∼1.5 MeV increase in temperature seen in the Natowitz compilation for $E^*/A = 2.5$–4.5. In this same region, the experimental data exhibit a ∼30% decrease in α/Δ. Therefore, the decrease in α/Δ in experimental data is not entirely explained by the drop in temperature, and there remains a portion that is reasonably associated with a density change with E^*/A.

To enhance our understanding of nuclear symmetry energy, experimentally determined values of temperature and density need to be extracted. Additionally, the experimental values of α obtained should be investigated for fragment secondary decay effects [33].

In conclusion, the present data of yield ratio distributions from ^{86,78}Kr + ^{64,58}Ni reactions at 35 MeV/nucleon exhibit excellent $Z = 1$–17 isoscaling over a broad range of isotopes with a consistent value of α. This consistency in α does not support a strong surface dependence of the nuclear symmetry energy. To accurately extract α from isoscaling, the N/Z of the source was well constrained and included free neutrons. The value of the α/Δ parameter exhibits a clear dependance on the excitation energy of the source. This dependance may indicate a decrease in the symmetry energy with increasing excitation energy.

The authors o thank the Texas A&M Cyclotron Institute staff for their support during the experiment. This work was supported by the US Department of Energy under Grant DE-FG03-93ER40773 and by the Robert A. Welch Foundation under Grant A1266.

[1] D. V. Shetty, S. J. Yennello, and G. A. Souliotis, Phys. Rev. C **76**, 024606 (2007).
[2] B. A. Li, L. W. Chen, and C. M. Ko, Phys. Rep. **464**, 113 (2008).
[3] V. Baran, M. Colonna, V. Greco, and M. Di Toro, Phys. Rep. **410**, 335 (2005).
[4] S. Kowalski *et al.*, Nucl. Phys. **A787**, 619 (2007).
[5] V. Greco *et al.*, Phys. Lett. **B562**, 215 (2003).
[6] B. A. Brown, G. Shen, G. C. Hillhouse, J. Meng, and A. Trzcinska, Phys. Rev. C **76**, 034305 (2007).
[7] H. S. Xu *et al.*, Phys. Rev. Lett. **85**, 716 (2000).
[8] G. Chaudhuri, S. Das Gupta, and M. Mocko, Nucl. Phys. **A813**, 293 (2008), and references therein.
[9] M. B. Tsang *et al.*, Phys. Rev. Lett. **86**, 5023 (2001).
[10] M. B. Tsang *et al.*, Phys. Rev. C **64**, 054615 (2001).
[11] M. B. Tsang *et al.*, Phys. Rev. C **64**, 041603(R) (2001).
[12] A. S. Botvina, O. V. Lozhkin, and W. Trautmann, Phys. Rev. C **65**, 044610 (2002).
[13] D. V. Shetty, S. J. Yennello, E. Martin, A. Keksis, and G. Souliotis, Phys. Rev. C **68**, 021602(R) (2003).
[14] G. A. Souliotis *et al.*, Phys. Rev. C **68**, 024605 (2003).
[15] S. R. Souza, M. B. Tsang, R. Donangelo, W. G. Lynch, and A. W. Steiner, Phys. Rev. C **78**, 014605 (2008).
[16] A. Ono, P. Danielewicz, W. A. Friedman, W. G. Lynch, and M. B. Tsang, Phys. Rev. C **68**, 051601(R) (2003).
[17] C. O. Dorso, C. R. Escudero, M. Ison, and J. A. Lopez, Phys. Rev. C **73**, 044601 (2006).
[18] S. Galanopoulos *et al.*, AIP Conf. Proc. **1099**, 786 (2009).
[19] S. Wuenschel *et al.*, Nucl. Instrum. Methods Phys. Res. A **604**, 578 (2009).
[20] S. Wuenschel *et al.*, AIP Conf. Proc. **1099**, 816 (2009).
[21] J. C. Steckmeyer *et al.*, Nucl. Phys. **A686**, 537 (2001).
[22] D. Lacroix, A. Van Lauwe, and D. Durand, Phys. Rev. C **69**, 054604 (2004).
[23] G. A. Souliotis *et al.*, Phys. Rev. C **73**, 024606 (2006).
[24] D. Rowland *et al.*, Phys. Rev. C **67**, 064602 (2003).
[25] M. Veselsky, G. A. Souliotis, and S. J. Yennello, Phys. Rev. C **69**, 031602(R) (2004).
[26] A. R. Raduta and F. Gulminelli, Phys. Rev. C **75**, 024605 (2007).
[27] G. A. Souliotis *et al.*, Phys. Rev. C **75**, 011601(R) (2007).
[28] D. Dore *et al.*, Phys. Lett. **B491**, 15 (2000).
[29] J. B. Natowitz *et al.*, Phys. Rev. C **65**, 034618 (2002).
[30] B. A. Li and L. W. Chen, Phys. Rev. C **74**, 034610 (2006).
[31] R. J. Charity *et al.*, Nucl. Phys. **A483**, 371 (1988).
[32] L. Tassan-Got and C. Stephan, Nucl. Phys. **A524**, 121 (1991).
[33] D. V. Shetty *et al.*, Phys. Rev. C **71**, 024602 (2005).